

# Experimental study of heat and mass transfer in convective flows of moist air with droplet condensation as a function of surface roughness and wetting properties

Andreas Westhoff<sup>1</sup>

<sup>1</sup> German Aerospace Center, Department Ground Vehicles, Göttingen, Germany

\* andreas.westhoff@dlr.de

## Abstract

Experiments are carried out in order to study the heat transfer in a forced convective air flow with phase transition on glass panes. The measurements are performed in a vertically oriented gap wind tunnel with a rectangular cross section. In addition, one side of the gap is isothermally cooled and a glass pane with a defined surface is mounted on the cooled wall. In the present paper the results of the heat and mass transfer are discussed as a function of the surface roughness and wetting properties for four different surfaces at a Reynolds number of  $Re = 2300$ . The heat transmission from the fluid through the glass pane and the corresponding mass transfer is examined in detail for one surface. The result reveals an impact of the droplet radius, vapour density and temperature on the heat transmission coefficient. Further, a linear relation between Sherwood  $Sh$  and Nusselt  $Nu$  for the present parameter variation is found. In addition, a non-dimensional parametrisation and an analysing method are introduced in order to characterise and determine the heat and mass transfer for the present configuration.

## 1 Introduction

Condensation and evaporation of droplets on an overflowed cool surface is a phenomenon which occurs in our everyday life, many technical applications, and nature. For instance, we are all familiar with the effect of misted windscreens in cars or the droplet condensation on the surface of heat exchangers (Aroussi et al. (2003)). The heat transfer in convective flows with moist air is determined by the physical mechanisms convection, phase transition and vapour diffusion as well as by the boundary conditions such as surface roughness and contact angle between the droplets and the surface. Moreover, during the phase change latent heat is released or consumed, which in turn influences the heat transfer (Talukdar et al. (2008); Nam and Ju (2013)). In particular the impact of surface roughness and the wetting properties on the mass transfer due to phase transition in mixed convective air flows is of vital interest for many applications. However, due to the mutual interplay of latent and sensible heat transfer in combination with forced convective flow, a simple characterisation of the present system is obviously doomed to failure. To overcome this problem the mechanisms of heat transfer regarding a rough surface are briefly described based on the analysis and considerations of Wenzel (1936) and Whyman et al. (2008), and a dimensionless characterisation of the present configuration is introduced.

The investigations are performed for a vertically oriented and overflowed glass pane with a defined surface which is cooled isothermally on one side (details see section 2). A schematic sketch of the physical processes determining the heat and mass transfer in case of condensation is depicted exemplarily in figure 1(a). Here, the moist air  $\partial u_x/\partial x$  enters the gap at the top and streams over a glass pane (shaded). The temperature of the cooled left side of the glass pane is  $T_b$ , while the temperature on the right side is  $T_g$ . If the temperature near the surface is below the dew point temperature  $\Theta$ , droplet condensation starts and latent heat is released. As a consequence, the temperature above the glass equals the saturation temperature  $T_{sat}$ . The corresponding heat transfer is  $\dot{Q} = \dot{M}H_v$ , where  $\dot{M}$  denotes the vapour mass flow due to phase transition and  $H_v$  the enthalpy of vaporisation. In addition to the latent heat, sensible heat is transported

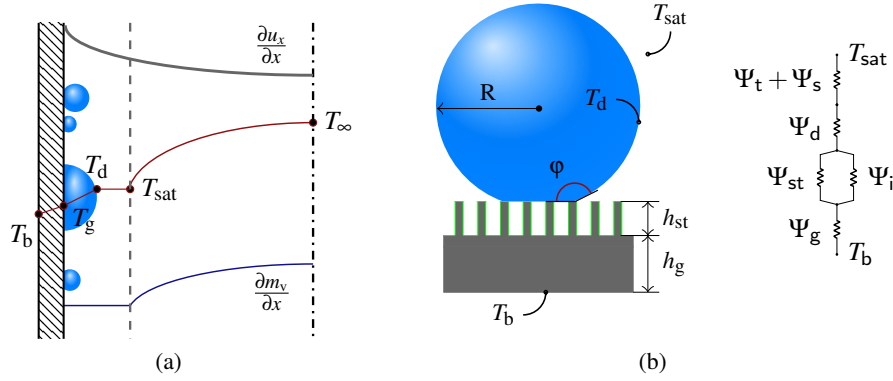


Figure 1: (a) A schematic sketch of the physical mechanism which determine the heat and the mass transport in case of moist air flow with droplet condensation on a cooled glass pane. (b) Droplet on a glass pane with a structured surface roughness and the corresponding heat resistance diagram which describes the heat transfer through the droplet.

by forced convection and heat conductance through the misted glass pane. The convective heat transfer is characterised by the flow properties while the heat conductance is a function of the thermal transmittance

$$k = \frac{1}{\Psi_t + \Psi_s + \Psi_d + \left(\frac{1}{\Psi_{st}} + \frac{1}{\Psi_i}\right)^{-1} + \Psi_g}, \quad (1)$$

where  $\Psi_t$  is the thermal resistance due the surface tension,  $\Psi_s$  the resistance between the air and the surface of the droplet (which is a function of the heat transfer coefficient  $\alpha$ , the radius  $R$  and the contact angle  $\phi$ ),  $\Psi_d$  the resistance resulting from the thermal conductivity of the droplet  $\lambda_w$  and  $\Psi_{st}$ ,  $\Psi_i$  and  $\Psi_g$  the resistances caused by the heat transfer through the surface structure, the interspace between the structure, and the glass pane, respectively. Figure 3(b) illustrates the heat transfer mechanisms and the corresponding heat resistance diagram. Finally, there is a third transport mechanism to be mentioned: the mass flow due to diffusion  $\dot{M} = -D_v \partial m_v / \partial x$ , where  $D_v$  is the diffusion coefficient of vapour and  $m_v$  the vapour mass density.

To describe such a complex system a set of non-dimensional parameters is defined, characterising the physical mechanisms of the present configuration. Basically, the set consists of six characteristic numbers: the Reynolds number  $\mathcal{R}e = U d_h \rho / \nu$ , the Prandtl number  $\mathcal{P}r = \nu / \lambda$ , the Froude number  $\mathcal{F}r = U / \sqrt{\Delta \rho / \rho g L}$ , the Jakob number  $\mathcal{J}a = \Delta T c_p / H_v$ , the Sherwood number  $\mathcal{S}h = |\Delta \dot{M}_v| H / W L D \Delta \rho_v$  and the Nusselt number  $\mathcal{N}u = \alpha L / \lambda$ . Here,  $U$  is the averaged inflow velocity,  $d_h$  the hydraulic diameter,  $L$  the length of the glass pane,  $\nu$  the kinematic viscosity,  $\rho$  the density of the moist air,  $\lambda$  the thermal conductivity,  $k$  the heat transmission coefficient (eq. 1),  $\Delta \rho$  the density difference of the moist air between the beginning and the end of the test section,  $\rho$  the mean density of the moist air,  $g$  the gravitational acceleration,  $\Delta T = T_s - T_w$  the temperature difference between the mean temperature of the moist air  $T_s$  and the cooled wall  $T_w$ ,  $c_p$  the specific heat capacity, and  $\Delta \rho_v$  the vapour density difference between the mean vapour density in the bulk and the saturation vapour density in the boundary near the glass pane surface. In addition, two non-dimensional parameters are needed to characterise the surface properties: the contact angle  $\phi$  and the surface roughness  $\varepsilon = R_z / H$  with  $R_z$  being the mean scallop height.

This set of non-dimensional parameters is applied to the experimental results in order to examine the scaling of the heat and mass transfer as a function of the surface roughness and the contact angle. In the following the results of heat and mass transfer of droplet condensation and evaporation on a cooled glass pane for one surface will be discussed in detail. Based on this discussion, the corresponding  $\mathcal{N}u - \mathcal{S}h$ -relation for four different surface is illustrated.

## 2 Test facility

The measurements were performed in a vertically oriented gap wind tunnel. Figure 2 depicts a sketch of the wind tunnel and the corresponding air supply system. The wind tunnel has a width of  $W = 529$  mm and a height of  $H = 20$  mm and consists of three sections: the inlet section with a length of  $L_i = 1500$  mm) in


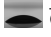


surface type	$R_z$ [nm]	$\epsilon = R_z/H$ [-]	contact angle	film gauge
hydrophobic	60	$0.3 \times 10^{-5}$	 $\bar{\varphi} = 101 \pm 2$	-
hydrophilic	60	$0.3 \times 10^{-5}$	 $\bar{\varphi} = 33 \pm 5$	-
polyester resin film I	230	$3.25 \times 10^{-5}$	 $\bar{\varphi} = 72 \pm 2$	$h = 71 \mu\text{m}$
polyester resin film II	650	$1.15 \times 10^{-5}$	 $\bar{\varphi} = 67 \pm 3$	$h = 75 \mu\text{m}$

Table 1: Listing of the surface properties of the glass panes including: surface roughness, contact angle and film gauge.

order to provide a fully developed flow, the test section ( $L_t = 2040$  mm) and the outflow section to ensure a well-defined outflow. All side-walls consist of acrylic glass except for the cooled side-wall in the test section. Here, a glass pane is mounted on an isothermally cooled aluminium plate. The different types of glass panes and corresponding surface properties such as roughness  $R_z$  and mean contact angle  $\bar{\varphi}$  of the droplets with the corresponding standard deviation are specified in table 1. The hydrophobic surface and the hydrophilic surface are implemented as coatings on the glass while the two types of roughness are realised by means of polyester resin films. All glass panes have a height of  $h_g = 10$  mm. Further, the inflow and outflow section are insulated to avoid thermal loss through the side-walls.

The corresponding air supply system includes a humidifier, a dryer, a radial blower and a heater. At the beginning of the air supply system dry and vapour-saturated air are mixed in a settling chamber. The moist air is sucked by the radial fan and is subsequently heated. To verify the mass and heat transport and to control the inflow conditions the test facility is equipped with a plethora of resistance thermometers (RTD) and humidity sensors. 23 RTDs are placed in the cooling plate to measure the mean wall temperature  $T_w$  as well as to control the wall temperature. In addition, four RTDs are located at the inlet of the inflow section to measure the mean inflow temperature  $T_i$  as well as at the outlet at the end of the outflow section for the validation of the mean outlet temperature  $T_o$ . The inflow temperature sensors are linked to the heater to control the inflow temperature. For the evaluation of the humidity four capacitive humidity sensors are positioned at the end of the air supply system ( $rH_i$ ) and at the outlet ( $rH_o$ ), respectively. To obtain a higher accuracy the humidity probes are calibrated at the beginning of each measurement by means of dew point mirrors. Based on these results, the mass transfer due to phase transition is calculated by the vapour mass flow difference between the inlet and the outlet  $\Delta \dot{M}_v = \dot{M}_v^i - \dot{M}_v^o$ . In addition, the humidity probes at the inlet are connected to the humidifier in order to control the humidity of the moist air. Further, the air supply system is equipped with a volume flow meter to measure and to control the volume flow  $\dot{V}$  of the moist air. With this system we are able to provide well-defined inflow and boundary conditions regarding volume flow, temperature and humidity.

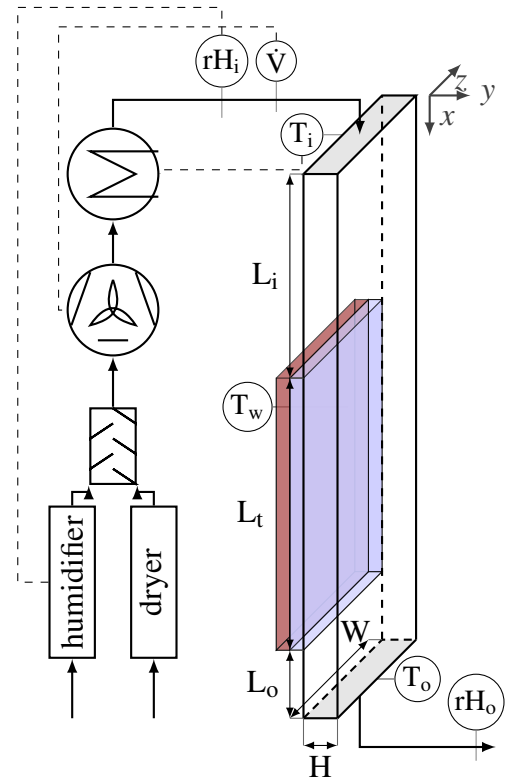


Figure 2: Schematic sketch of the gap wind tunnel and the air supply system.

### 3 Results

With the aim to ensure well-defined and reproducible condensation and evaporation on the cooled glass pane the measurements are performed under constant inflow conditions and varying wall temperatures. For the

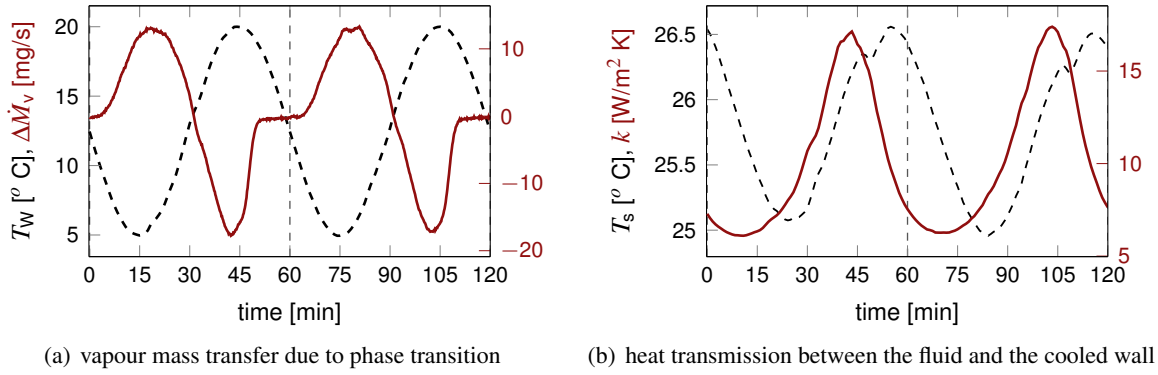


Figure 3: Heat and mass transfer as a function of time: (a) vapour mass transfer  $\Delta\dot{M}_v$  and wall temperatures  $T_w$  and (b) heat transmission coefficient  $k$  and mean system temperature  $T_s$ .

present investigation the inflow parameters are the dew point temperature  $\Theta_i = 11^\circ \text{C}$ , the mean velocity of the moist air  $U = 1.0 \text{ m/s}$  and the inflow temperature  $T_i = 32.5^\circ \text{C}$ , while the varying mean wall temperatures is given by the sinusoidal function  $T_w = 12.5^\circ\text{C} + 7.5^\circ\text{C} \cdot \cos\left(2\pi \frac{t+900\text{s}}{\tau}\right)$ , where  $\tau = 60 \text{ min}$  is a measurement period. The temporal resolution of the measurement is 10 s. To illustrate the physical processes, which determine the vapour mass transfer and the global heat transfer for the present configuration, results for the surface polyester resin film I are outlined in figure 3.

Figure 3(a) shows the resulting vapour mass transfer  $\Delta\dot{M}_v$  as a function of time for two measurement periods, where positive values indicate condensation and the negative values evaporation. The dashed black line depicts the wall temperature  $T_w$  and the red solid line the vapour mass transfer. If the wall temperature falls below the point temperature  $\Theta_i = 11^\circ \text{C}$ , the process of condensation on the glass pane starts. With decreasing  $T_w$  an increase of vapour mass flow is found. Similarly the process of evaporation runs when  $T_w$  exceeds the dew point temperature  $\Theta_i = 11^\circ \text{C}$ . At the end of each measurement period the total water on the glass pane is evaporated and the temperature is above the dew point. Hence, no vapour mass transfer is indicated. This ensures that at the beginning of the next measurement period no water is on the glass surface. Two effects are found by analysing the relation of wall temperature and vapour mass transfer. The first effect is that the onset of condensation and evaporation does not occur directly with falling below or exceeding the dew point temperature  $\Theta_i = 11^\circ \text{C}$ , respectively. One reason for the delayed onset results obviously from the insulation effect of the glass pane. The other participating effect is the additional latent heat, which has to be transported through the glass pane by heat conduction or by the fluid flow via convection. The second effect is that the process of evaporation runs faster compared to condensation. Here, the time in which the same amount of water evaporates - that condensed on the glass pane before - is significantly shorter compared to the period of condensation. The reason for the difference is that the latent heat during the condensation is primarily transported through the glass pane by conduction. This is slower than the convective heat transfer which is dominant in case of evaporation.

In addition, figure 3(b) depicts the corresponding mean system temperature  $T_s$  as well as the mean heat transmission coefficient  $k$  between the fluid and the cooling plate. The calculation of both parameters is based on the differential equation

$$\frac{dT}{dx} = \frac{1}{c_p \dot{V} \rho} \left( \underbrace{W k (\mathbf{T}(\mathbf{x}) - T_w)}_{\dot{Q}_w} + \underbrace{(2H + W) k_{sw} (\mathbf{T}(\mathbf{x}) - T_a)}_{\dot{Q}_{sw}} + \underbrace{\Delta\dot{M}_v H_v}_{\dot{Q}_l} \right), \quad (2)$$

which represents the global thermal balance including the heat flux between the fluid and the cooled wall  $\dot{Q}_w$ , the heat loss through the acrylic glass side walls  $\dot{Q}_{sw}$  and the latent heat  $\dot{Q}_l$ , where  $k_{sw}$  is the heat transmission coefficient for the heat loss through the acrylic glass side walls and  $T_a$  the ambient temperature in the vicinity of the test section. Equation 2 is solved for each time step using an iterative algorithm which depends on varying  $k$  and  $T_w$  on the condition that  $T(x=L)$  equals the measured mean outflow temperature  $T_o$ . Hence, we obtain the mean temperature  $T_s(x)$  of the horizontal cross section in function of the flow direction  $T(x)$  for each measurement point. A complete introduction of the method would go beyond the scope of this paper, however, details are published in Westhoff (2017).

The calculated system temperature  $T_s = \int T_s(x) dx$  and the mean heat transmission coefficient are shown in figure 3(b) as a function of time. Similar to  $T_w$ , the temperature  $T_s$  is a sinus function, but the minimum

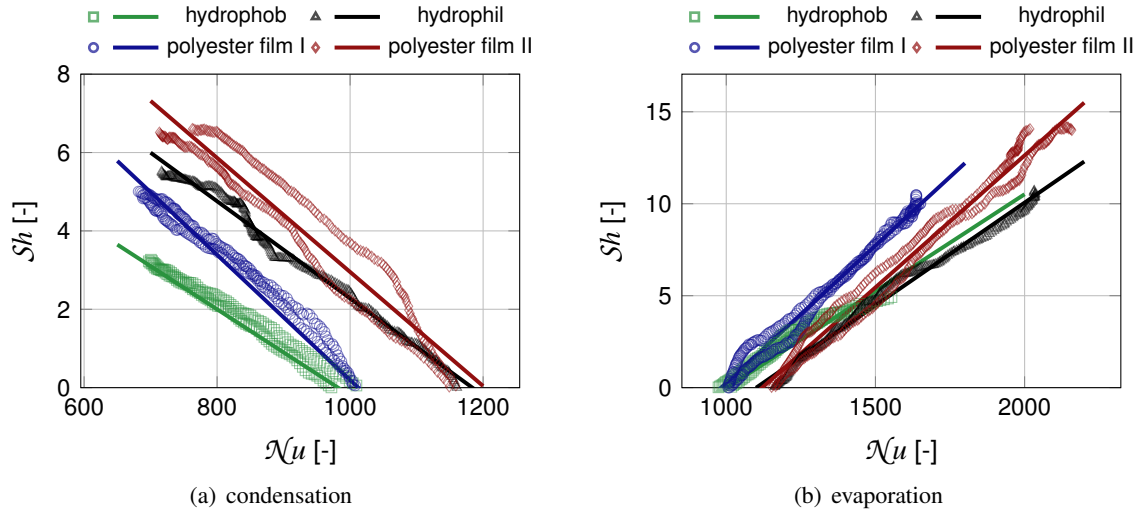


Figure 4:  $Sh$  as a function of  $Nu$  for the four different surfaces: hydrophobic, hydrophilic, polyester resin film I ( $\epsilon = 3.25 \times 10^{-5}$ ) and polyester resin film II ( $\epsilon = 1.15 \times 10^{-5}$ ) at  $Re = 2300$  in case of condensation (a) and evaporation (b).

and maximum of  $T_s$  are delayed by  $t \approx 10$  min with regard to  $T_w$  (fig. 2). The delay is caused by the heat transport through the glass pane as well as by the release and consumption of the latent heat. Further, a discontinuity of the sinusoidal behaviour of  $T_s$  is found for  $t \approx 50$  min and  $t \approx 110$  min, revealing the time on which the total water mass is evaporated. For the heat transmission coefficient  $k$  a decrease is found at the beginning with a minimum shortly after the process of condensation starts. At the beginning of the condensation process just a small number of droplets is formed at the end of the test section which results in a higher heat resistance on the cooled surface. Further, the reduced heat conductivity of the air  $\lambda$  at decreased temperatures leads additionally to lower value of  $k$ . With growing droplets on the glass pane and rising temperature  $T_w$  the heat transmission coefficient  $k$  increases and reaches its maximum shortly before  $T_w$  is maximal. Due to the mutual interplay of sensible and latent heat transfer the reason for the increase of  $k$  during the process of condensation and evaporation cannot be attributed to a single effect. Primarily, there are three effects that can be assumed to result in an increase of  $k$ . In the period of rising  $k$  the air in the boundary layer above the cooled glass pane is saturated. As a consequence, the increasing wall temperature leads to an increase of vapour density in the boundary layer which results in a higher heat conductivity  $\lambda$  of the air and thus in rising values of  $k$ . Further, the thermal resistance on the droplet surfaces  $\Psi_t$ , the heat transfer between air and droplet  $\Psi_s$ , and the heat resistance of the droplets  $\Psi_d$  are proportional to the droplet radius  $R^{-1}$  and  $R^{-2}$ . As a result,  $k$  increases with increasing  $R$  in case of condensation. The continuing increase of  $k$  during the process of evaporation seems to be the result of the additional vapour which evaporates into the fluid and the rising wall temperature  $T_w$ . Both effects lead to a higher vapour density of the fluid and thus to a higher heat conductivity of the air which once again results in a rising heat transmission  $k$ . With falling  $T_w$  and the resulting lower vapour mass transfer due to evaporation and thus the lower vapour density as well, the heat transmission  $k$  decreases and once again reaches a minimum at the beginning of the condensation process.

Based on the calculation discussed before,  $Sh$  and  $Nu$  are determined for the four surfaces.  $Sh$  is the measure for vapour mass transport to or away from the glass pane. It represents the ratio of vapour mass flow due to phase transition to diffusive vapour mass transport.  $Nu$  is a measure of the total heat transfer including convective, conductive and latent heat transfer. For the calculation of  $Nu$ , the heat transfer coefficient between the misted glass pane and the air is  $\alpha = (1/k - d_g/\lambda_g - d_f/\lambda_f)^{-1}$ , where  $d$  and  $\lambda$  are the thickness and heat conductivity of the glass pane and the polyester film respectively. Figure 4 shows  $Sh$  as a function of  $Nu$  in case of condensation (fig. 4(a)) and evaporation (fig. 4(b)) for  $Re \approx 2300$ . Each data point reveals the result for a single measuring point of two measurement periods. However, for the sake of visibility just every sixth point is illustrated. Additionally, it should be noted that here just the period is shown in which the total glass pane is misted. For the present parameters an almost linear relation  $Sh = mNu + b$  is found. This result underpins the mutual dependency of latent and sensible heat transport. In case of

condensation similar slopes  $m$  are found for the surfaces with the lower roughness values  $\varepsilon$  (hydrophobic  $m = -0.011$  and hydrophilic  $m = -0.012$ ) and for the higher roughness values (polyester film I  $m = -0.016$  and polyester film II  $m = -0.015$ ). Further, clear differences of the heat and mass transfer are detected. The  $Sh$  of the hydrophobic surface is significantly lower compared with the other surfaces. This means, that for a comparable diffusive vapour mass flow a lower vapour mass transfer due to phase transition is obtained for the same  $\mathcal{N}u$ . This is equivalent to a lower condensation rate on the glass surface. Based on the same argument, elevated condensation is found in case of the polyester film II. This interpretation is in agreement with the result that in case of the hydrophobic surface the lowest total water mass is found and in case of polyester film II the highest. In case of evaporation similar slopes  $m$  are found also for the surfaces with the lower roughness (hydrophobic  $m = 0.011$  and hydrophilic  $m = 0.011$ ) and for the higher roughness (polyester film I  $m = 0.015$  and polyester film II  $m = 0.014$ ). Here, the highest  $Sh$  for a given  $\mathcal{N}u$  are found for the polyester film I and the lowest for the hydrophilic surface.

## 4 Conclusion

The study presents an experimental investigation on the heat and mass transfer in forced convective air flow with phase transition on a misted glass pane as a function of the roughness and the wetting properties. In the introduction the physical basics are illustrated which determine the transfer processes for the present configuration. Based on these considerations a set of non-dimensional parameters is introduced in order to characterises the system. The measurements are performed in a vertically oriented gap wind tunnel with a cooled side wall on which different types of glass panes are mounted. The study of the heat transmission between the fluid and the cooled wall through the glass pane reveals two predominant factors influencing the heat transfer: the droplet shape characterised by the radius  $R$  and the heat conductivity of the moist air which is a function of the vapour density as well as the mean temperature of the wall and the system. An analysis of the  $Sh$ - $\mathcal{N}u$  relation for the four different surfaces discloses a linear relation for the present parameter variation. Here, the surfaces with lower and higher roughness have similar slopes.

## Acknowledgements

This research has been funded by the German Association of the Automotive Industry (VDA) in the project experimental study of condensation on glass panes as a function of surface properties.

## References

- Aroussi A, Hassan A, and Morsi Y (2003) Numerical simulation of the airflow over and heat transfer through a vehicle windshield defrosting and demisting system. *Heat and Mass Transfer* 39:401–405
- Nam Y and Ju YS (2013) A comparative study of the morphology and wetting characteristics of micro/nanostructured cu surfaces for phase change heat transfer applications. *Journal of Adhesion Science and Technology* 27:2163–2176
- Talukdar P, Iskra CR, and Simonson CJ (2008) Combined heat and mass transfer for laminar flow of moist air in a 3d rectangular duct: Cfd simulation and validation with experimental data. *International Journal of Heat and Mass Transfer* 51:3091–3102
- Wenzel RN (1936) Resistance of solid surfaces to wetting by water. *Industrial & Engineering Chemistry* 28:988–994
- Westhoff A (2017) Experimental study of condensation on glass panes as a function of surface properties. *FAT-Series VDA* 303
- Whyman G, Bormashenko E, and Stein T (2008) The rigorous derivation of young, cassie–baxter and wenzel equations and the analysis of the contact angle hysteresis phenomenon. *Chemical Physics Letters* 450:355–359